

## Pion Production in Antiproton-Proton Annihilations at 3.3 and 3.7 BeV/c\*

T. FERBEL,<sup>†</sup> A. FIRESTONE, J. SANDWEISS,<sup>‡</sup> AND H. D. TAFT  
*Yale University, New Haven, Connecticut*

AND

M. GAILLOUD,<sup>§</sup> T. W. MORRIS, AND W. J. WILLIS||  
*Brookhaven National Laboratory, Upton, New York*

AND

A. H. BACHMAN, P. BAUMEL, AND R. M. LEA  
*The City College of New York, New York, New York*  
 (Received 11 November 1965)

A study of antiproton-proton collisions at 3.3 and 3.7 BeV/c indicates that (41±4)% of the total interaction cross section can be attributed to annihilation into pions. The average pion multiplicity is 6.5±0.5. The positively charged pions and dipions tend to be emitted backward, while the negatively charged pions and dipions tend to be emitted forward in the center-of-mass system. Although there is a substantial amount of resonance production, especially of  $\rho$  and of  $\omega$  mesons, there is no clear evidence for double or associated resonance production in these final states. A search for new resonances as well as for some of the recently discovered mesons proved unsuccessful.

### I. INTRODUCTION

THIS paper is one in a series of reports which present the results of a bubble-chamber investigation of antiproton-proton interactions at 3.3 and 3.7 BeV/c. The specific topics covered here are the multiple-pion final states resulting from  $\bar{p}$ - $p$  annihilations. The previous reports dealt with the experimental details concerning the antiproton beam, elastic scattering, and a summary of major cross sections,<sup>1</sup> pion production without annihilation<sup>2</sup>; and the production of kaons<sup>3</sup> and hyperons.<sup>4</sup> These studies utilized pictures obtained in an exposure of the BNL 20-in. liquid-hydrogen bubble chamber to separated antiproton beams of momenta 3.28 BeV/c<sup>5</sup> and 3.66 BeV/c at the Alternating Gradient Synchrotron (AGS).

The results of this paper are based on an analysis of approximately 1400 two-pronged stars, 8000 four-

\* Work partially supported by the U. S. Atomic Energy Commission and the National Science Foundation.

<sup>†</sup> Present address: University of Rochester, Department of Physics and Astronomy, Rochester, New York.

<sup>‡</sup> Alfred P. Sloan Foundation Fellow.

<sup>§</sup> Present address: Laboratory of Nuclear Research, Ecole Polytechnique, Lausanne, Switzerland.

|| Present address: Yale University, Department of Physics New Haven, Connecticut.

<sup>1</sup> T. Ferbel, A. Firestone, J. Sandweiss, H. D. Taft, M. Gaillard, T. W. Morris, A. H. Bachman, P. Baumel, and R. M. Lea, *Phys. Rev.* **137**, B1250 (1965).

<sup>2</sup> T. Ferbel, A. Firestone, J. Sandweiss, H. D. Taft, M. Gaillard, T. W. Morris, W. J. Willis, A. H. Bachman, P. Baumel, and R. M. Lea, *Phys. Rev.* **138**, B1528 (1965).

<sup>3</sup> C. Baltay, J. Lach, J. Sandweiss, H. D. Taft, N. Yeh, D. L. Stonehill, and R. Stump, *Phys. Rev.* **142**, 932 (1966).

<sup>4</sup> C. Baltay, J. Sandweiss, H. D. Taft, B. B. Culwick, J. Kopp, R. Louttit, R. P. Shutt, A. M. Thorndike, and M. S. Webster, *Phys. Rev.* **140**, B1027 (1965).

<sup>5</sup> For a brief discussion of these data at 3.28 BeV/c see C. Baltay, T. Ferbel, J. Sandweiss, H. D. Taft, B. B. Culwick, W. B. Fowler, M. Gaillard, J. K. Kopp, R. I. Louttit, T. W. Morris, J. R. Sanford, R. P. Shutt, D. L. Stonehill, R. Stump, A. M. Thorndike, M. S. Webster, W. J. Willis, A. H. Bachman, P. Baumel, and R. M. Lea, *Nucleon Structure* (Stanford University Press, Stanford, California, 1964), pp. 275-278. Also T. Ferbel, thesis, Yale University, 1963 (unpublished).

pronged stars, 2000 six-pronged stars, and 300 eight-pronged stars.<sup>6</sup> The final states considered are listed in Table I. The major portion of this work is concerned with the four-pronged and six-pronged events.

The methods used in the classification of events and a summary of the cross sections for the reactions in Table I are given in Sec. II. Section III deals with angular distributions. In Sec. IV effective-mass distributions are presented with particular emphasis on production cross sections for resonant states which decay into pions.

TABLE I.  $\bar{p}$ - $p$  annihilations into pions.

Reaction	Final state	Cross section <sup>a</sup> at 3.28 BeV/c (mb)
Two-pronged stars		
(1)	$\pi^-\pi^+$	<0.025
(2)	$\pi^-\pi^+\pi^0$	0.5 ± 0.2
(3)	$\pi^-\pi^+n\pi^0 (n \geq 2)$	6.7 ± 2.2
Four-pronged stars		
(4)	$2\pi^-2\pi^+$	0.8 ± 0.1
(5)	$2\pi^-2\pi^+\pi^0$	4.5 ± 0.6
(6)	$2\pi^-2\pi^+n\pi^0 (n \geq 2)$	12.0 ± 1.2
Six-pronged stars		
(7)	$3\pi^-3\pi^+$	0.9 ± 0.1
(8)	$3\pi^-3\pi^+\pi^0$	2.7 ± 0.3
(9)	$3\pi^-3\pi^+n\pi^0 (n \geq 2)$	2.4 ± 0.5
Eight-pronged stars		
(10)	$4\pi^-4\pi^+$	0.10 ± 0.03
(11)	$4\pi^-4\pi^+\pi^0$	0.25 ± 0.06
(12)	$4\pi^-4\pi^+n\pi^0 (n \geq 2)$	~0.1
Total		30.9 ± 3.0

<sup>a</sup> For corrections applied to reactions (3) and (6) due to kaon and nucleon contamination see the data contained in Tables I and II in Ref. 1, and Table II in Ref. 2.

<sup>6</sup> The two-pronged and the six-pronged data were obtained at 3.28 BeV/c. Four-pronged and eight-pronged data came largely from the sample at the higher energy (about 30% of the events measured were at 3.28 BeV/c). The distributions at the two energies were not sufficiently different to warrant separate treatment. In what follows no distinction is made between the samples obtained at the two energies; the cross sections, however, are given only for 3.28 BeV/c. For an early treatment of the data at 3.28 BeV/c, see Ref. 5.

## II. IDENTIFICATION OF EVENTS AND CROSS SECTIONS

### A. Four-Pronged and Six-Pronged Stars

The production hypotheses involving annihilation into pions which were considered for each of the four-pronged stars were reactions (4), (5), and (6) in Table I; while for six-pronged stars reactions (7), (8), and (9) were considered. In order to obtain a reliable sample of events for a study of reactions (4), (5), (7), and (8) the following acceptance criteria were applied to the data: (a). Kinematic consistency was required with the four-constraint<sup>7</sup> interpretation in the case of reactions (4) and (7) or with the one-constraint interpretation in the case of reactions (5) and (8); and (b) kinematic or ionization inconsistency was required with (i) the four- and one-constraint reaction hypotheses involving pion production without annihilation<sup>2</sup> (e.g.,  $\bar{p}+p \rightarrow \bar{p}+p+\pi^-+\pi^+$  or  $\bar{p}+p \rightarrow \bar{p}+p+\pi^-+\pi^++\pi^0$ ), and (ii) the four-constraint reaction hypotheses involving annihilation into kaons and pions<sup>3</sup> (i.e.,  $\bar{p}+p \rightarrow K^-+K^++\pi^-+\pi^+$ ). Dalitz pairs from the decay of  $\pi^0$  mesons were eliminated by removing events with low effective masses for minimum ionizing positive-negative pairs of tracks.

Those four-pronged events which met criterion (b) but failed (a) and for which the missing momentum was  $>200$  MeV/c and the missing mass was  $>0$  were classified as reaction (6); similar six-pronged events were classified as reaction (9). The purpose of this missing-mass and momentum restriction was to reduce the background in the nonfitted samples from events that had incorrect mass interpretations or that were measured incorrectly. Similar considerations for reactions (5) and (8) led to the criterion that, for acceptable fits to these reactions, the cosine of the production angle of the  $\pi^0$  in the center-of-mass system be greater than  $-0.96$  for reaction (5) and greater than  $-0.98$  for reaction (8).<sup>8</sup>

<sup>7</sup> J. P. Berge, F. T. Solmitz, and H. Taft, Rev. Sci. Instr. **32**, 538 (1961).

<sup>8</sup> It was found that events which were identifiable on the basis of ionization as four-constraint nucleon or kaon interpretations often made acceptable fits to the one-constraint annihilation hypothesis. These misinterpreted events all made the one-constraint fit with a characteristically backward  $\pi^0$  in the center-of-mass system. This result is understandable because in making this incorrect fit the program CUTS (see Ref. 7) introduces a slow  $\pi^0$  in the laboratory which is equivalent to a  $\pi^0$  going strongly backward in the center-of-mass system. Upon removing the identified four-constraint nonannihilation fits from the annihilation events a small backward peak in the  $\pi^0$  angular distribution in the center-of-mass system still remained. The source of this backward peak is not fully understood; it has been assumed to be due to mismeasured four-constraint events or those four-constraint events caused by a known  $\pi^-$  contamination in the antiproton beam. Note that if the sharp backward peaks in the  $\pi^0$  production angular distributions are real they violate  $C$  invariance in the  $\bar{p}$ - $p$  strong interactions. Hence the  $\pi^0$ -production-angle criteria were applied to eliminate this asymmetric background; the cross sections were corrected for the small number of real events which were lost owing to these cutoffs ( $\sim 2\%$ ).

The contamination of the samples for reactions (4) and (7) which arises from the final states involving nucleons or kaons is insignificant in view of the kinematically overdetermined nature of these two reactions, and the use of the ionization criteria. The amount of this type of background in the samples for reactions (5) and (8) is small<sup>9</sup> and relatively unimportant when compared with the major contamination in these samples, namely, the background from reactions (6) and (9). This background is due to the fact that measuring errors are large. For example the uncertainty in the missing mass for these events is of the order of one to two pion masses. The  $\chi^2$  criterion that was used to classify the single- $\pi^0$  samples admitted an estimated 20% contamination from the multiple- $\pi^0$  reactions in reaction (5) and an 8% contamination in the case of reaction (8). The method used in obtaining these estimates is illustrated in Fig. 9. The Lorentz-invariant phase-space prediction for the  $\pi^\pm\pi^\pm\pi^\mp$  invariant-mass distribution in the  $2\pi^++2\pi^-+\pi^0$  final state [curve (b) in that figure] is not in agreement with the experimental distribution. A varying fraction of the  $6\pi$  phase-space curve (i.e., for the reaction  $2\pi^-+2\pi^++2\pi^0$ ) was added to the  $5\pi$  curve in order to obtain a reasonable fit to the experimental distribution. This was done for several invariant-mass distributions for the events of reaction (5) and the best over-all fit was obtained for an 80%  $5\pi$  and 20%  $6\pi$  combination.<sup>10</sup>

### B. Two-Pronged and Eight-Pronged Stars

An attempt was made to fit a sample of approximately 1400 two-pronged stars, found in a restricted region of the bubble chamber, to reactions (1) and (2). None of these events made a kinematic fit to the four-constraint hypothesis [reaction (1)]. The large measuring errors enabled many events which were non-annihilations to kinematically fit the one-constraint hypothesis [reaction (2)]. It was therefore necessary to examine each event for ionization consistency in order to obtain estimates of the cross sections for reactions (2) and (3).

Eight-pronged events in which at least one of the tracks was identified as an electron by ionization were removed from the sample of 300 eight-pronged stars. The remaining events were classified as reactions (10),

<sup>9</sup> An upper limit for this contamination is 5%. This limit results from the application of criterion (b) and the much smaller relative cross section for the remaining channels in which there is a nucleon or nondecaying kaon in the final state (see Refs. 2 and 3).

<sup>10</sup> This estimate of the multi- $\pi^0$  contamination in reaction (5) is somewhat uncertain because the effect of the fitting process on the multi- $\pi^0$  events was not taken into account. An independent determination was therefore obtained by generating four-pronged events by using four of the six outgoing tracks of the sample of reaction (7), processing these events through the same kinematic fitting program used to obtain the reaction (5) sample, and determining the fraction of events for which an acceptable  $\chi^2$  was obtained for the reaction (5) hypothesis. The background estimates obtained using this method were in good agreement with the results from the comparison of mass spectra. Also see Sec. IV.

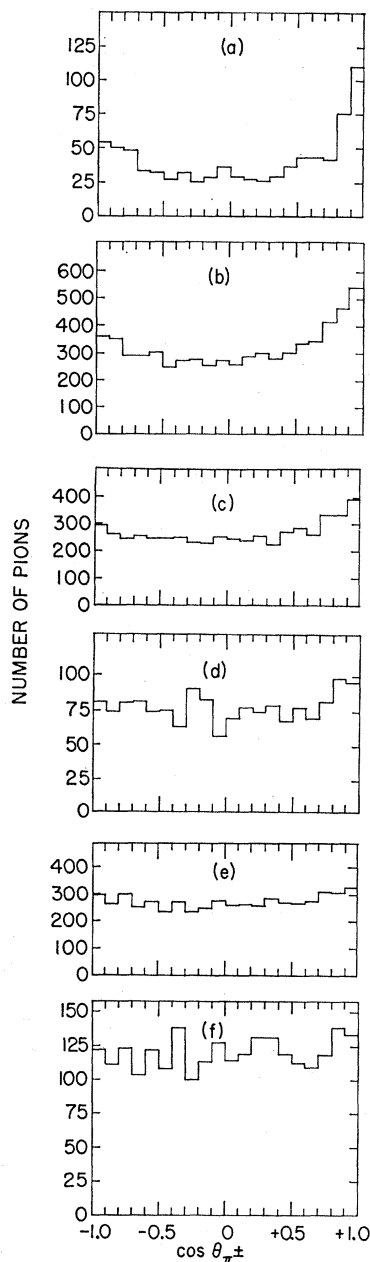


FIG. 1. Distributions of the production angles of charged pions in the center-of-mass system.  $\theta_{\pi^{\pm}}$  is the angle of the  $\pi^+$  with respect to the proton and that of the  $\pi^-$  with respect to the antiproton direction. (a) 216 events of reaction (4); (b) 1596 events of reaction (5); (c) 1334 events of reaction (6); (d) 255 events of reaction (7); (e) 906 events of reaction (8), and (f) 399 events of reaction (9).

(11), or (12) on the basis of  $\chi^2$  criteria alone. These simple procedures were sufficient to obtain a separation of the three final states because of the considerably smaller uncertainty in the missing mass in the eight-pronged events ( $\sim 50$  MeV) as compared with that in the lower charged-pion multiplicities.

### III. ANGULAR DISTRIBUTIONS

Three kinds of angular distributions have been studied in this experiment: production angles of pions ( $\theta_{\pi}$ ) and dipions ( $\theta_d$ ) in the center-of-mass system; angles between the momentum vectors of two pions in

the center-of-mass system ( $\theta_{\pi,\pi}$ ); and the decay angular distributions of dipions in their own rest frames ( $\theta_{\pi,d}$ ).

#### A. Production Angles in the Center-of-Mass System

Invariance of  $\bar{p}$ - $p$  strong interactions under charge conjugation requires that the distribution of  $\theta_{\pi^-}$  be the same as that of  $\theta_{\pi^+}$  if the direction of the  $\pi^+$  is computed with respect to the incoming proton direction.<sup>11</sup> Our data are consistent with this assumption, and the two distributions have therefore been combined in the same plots.<sup>12</sup> Figure 1 shows the angular distributions in the center of mass for charged pions in reactions (4) through (9). The data indicate that the  $\pi^-(\pi^+)$  tend to be emitted in the direction of the incoming  $\bar{p}(p)$ . This asymmetry, which has been noted previously at 1.61 BeV/c,<sup>13</sup> can be described by the  $(F-B)/(F+B)$  ratio ( $F$  is the number of pions with  $\cos\theta_{\pi} > 0.0$ ;  $B$  is the number with  $\cos\theta_{\pi} < 0.0$ ). These ratios, along with  $(P-E)/(P+E)$  ratios for the data in Fig. 1 ( $P$  is the number of pions with  $|\cos\theta_{\pi}| > 0.5$ ,  $E$  is the number with  $|\cos\theta_{\pi}| < 0.5$ ) are given in Table II. The table clearly indicates that the anisotropy decreases with increasing multiplicity. The anisotropy also appears to increase with increasing energy.<sup>31,14</sup>

Figure 2 gives the distributions of  $\theta_{\pi^0}$  for reactions

TABLE II. Forward ( $F$ ) to backward ( $B$ ) and polar ( $P$ ) to equatorial ( $E$ ) comparisons for pion production angles in the center-of-mass system.

Reaction	Charged pions		Neutral pions <sup>a</sup>
	$(F-B)/(F+B)$	$(P-E)/(P+E)$	$(P-E)/(P+E)$
(4)	$0.115 \pm 0.033$	$0.285 \pm 0.030$	...
(5)	$0.119 \pm 0.014$	$0.153 \pm 0.014$	$0.17 \pm 0.03$
(6)	$0.070 \pm 0.008$	$0.071 \pm 0.008$	...
(7)	$0.052 \pm 0.040$	$0.039 \pm 0.040$	...
(8)	$0.068 \pm 0.026$	$0.113 \pm 0.026$	$-0.06 \pm 0.07$
(9)	$0.043 \pm 0.024$	$0.011 \pm 0.026$	...
(10)	$0.004 \pm 0.046$	$-0.055 \pm 0.046$	...
(11)	$0.063 \pm 0.031$	$-0.056 \pm 0.031$	$-0.02 \pm 0.09$
(12)	$0.014 \pm 0.059$	$0.000 \pm 0.059$	...

<sup>a</sup> Corrections were applied due to the presence of biases in the data. See Ref. 8.

<sup>11</sup> A. Pais, Phys. Rev. Letters **3**, 242 (1959).

<sup>12</sup> Similarly, the distributions in  $\theta_d$  for positively charged dipions when measured with respect to the proton line of flight are consistent with the  $\theta_d$  for the negative dipions (of same charge magnitude) when these are measured with respect to the antiproton line of flight in the center of mass. A dipion angle  $\theta_d$  is defined by the direction of the vector sum of the two-pion momenta which make up that dipion.

<sup>13</sup> B. C. Maglic, G. R. Kalbfleisch, and M. L. Stevenson, Phys. Rev. Letters **7**, 137 (1961); N. Xuong and G. Lynch, Phys. Rev. **128**, 1849 (1962). The average  $F/B$  ratio in the four prongs at 1.61 BeV/c is given as  $1.13 \pm 0.03$ . This is to be compared with  $1.21 \pm 0.02$  at 3-4 BeV/c. The six prongs at 1.61 BeV/c are consistent with no asymmetry.

<sup>14</sup> T. Ferbel, A. Firestone, J. Johnson, J. Sandweiss, and H. D. Taft, Nuovo Cimento **38**, 12 (1965). At 7 BeV/c the  $F/B$  ratio for reaction (8) is  $1.31 \pm 0.10$  while at 3-4 BeV/c it is  $1.14 \pm 0.07$ .

(5) and (8). Both distributions are symmetric about  $90^\circ$ .<sup>8</sup> This is a consequence of the fact that the  $\pi^0$  and its antiparticle are indistinguishable. The  $\pi^0$ 's are also emitted preferentially in the forward and backward directions.

The anisotropy of the charged and neutral pions can perhaps be understood by considering a qualitative extension of the Koba-Takeda model<sup>15</sup> to annihilations in flight. In this model the nucleon consists of a core and a cloud of pions. The proton cloud has a net positive charge while the antiproton cloud has a net negative charge but both clouds contain all three charge states of the pion. In  $\bar{p}p$  annihilation the cores annihilate and emit pions isotropically while the cloud pions continue to move with their original momenta. Thus, the forward peaking in Fig. 1 is interpreted as being due to the excess of  $\pi^-$  over  $\pi^+$  in the  $\bar{p}$  cloud (and the excess  $\pi^+$  in the  $p$  cloud) while the smaller backward peaking may be understood as arising from the  $\pi^-$  emitted by the proton cloud and the  $\pi^+$  emitted by the antiproton cloud. Similarly, the  $\pi^0$  peaking arises from the neutral pions in the clouds.

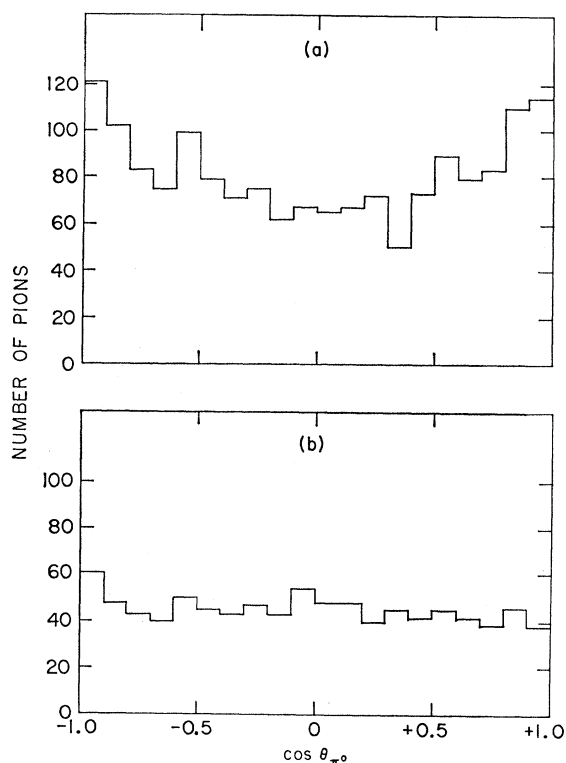
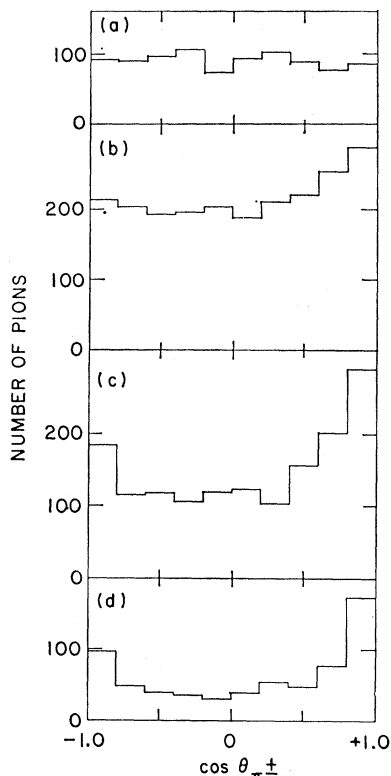


FIG. 2. Distributions of the production angles of the neutral pions,  $\theta_{\pi^0}$  for (a) reaction (5) and (b) reaction (8). The  $\pi^0$  production angle is with respect to the direction of the antiproton. The most backward bin has been corrected for losses due to a cutoff on the production angle of the  $\pi^0$ . (See footnote 8.)

<sup>15</sup> Z. Koba and G. Takeda, Progr. Theoret. Phys. (Kyoto) **19**, 269 (1958).

FIG. 3. Distributions of the production angles of the charged pions of reaction (5) in the center-of-mass system versus their momentum. The angle of the  $\pi^+$  is with respect to the proton, while that of the  $\pi^-$  is with respect to the antiproton direction. The momentum regions are (a) 0–300 MeV/c; (b) 300–600 MeV/c; (c) 600–900 MeV/c, and (d) 900–1400 MeV/c.



In the extended Koba-Takeda model of Stajano<sup>16</sup> and in a statistical model discussed by Pilkuhn<sup>17</sup> a prediction is made that the pion-angular asymmetry depends strongly on the momentum of the pion in the center-of-mass system. In Fig. 3 the distribution of  $\theta_{\pi^\pm}$  from reaction (5) is plotted for several ranges of  $\pi^\pm$  momentum. The  $(F-B)/(F+B)$  ratio is  $-0.01 \pm 0.03$  for pion momenta below 300 MeV/c while it is  $0.22 \pm 0.04$  for pion momenta above 900 MeV/c. As predicted, the asymmetry is particularly characteristic of the faster pions in the center-of-mass system.

Dipion production angular distributions for reactions (5) and (8) are given in Fig. 4.<sup>12</sup> These distributions in

TABLE III. Forward ( $F$ ) to backward ( $B$ ) and polar ( $P$ ) to equatorial ( $E$ ) comparisons for dipion production angles in the center-of-mass system.

Reaction	Dipion charge	$(F-B)/(F+B)$	$(P-E)/(P+E)$
(5)	0	$-0.012 \pm 0.013^a$	$0.187 \pm 0.012$
	1	$0.089 \pm 0.013$	$0.174 \pm 0.012$
	2	$0.168 \pm 0.016$	$0.185 \pm 0.016$
(8)	0	$0.015 \pm 0.012^a$	$0.099 \pm 0.011$
	1	$0.037 \pm 0.014$	$0.076 \pm 0.014$
	2	$0.088 \pm 0.014$	$0.062 \pm 0.014$

<sup>a</sup> Required to be zero if reaction is invariant under  $C$ .

<sup>16</sup> A. Stajano, Nuovo Cimento **28**, 197 (1963).

<sup>17</sup> H. Pilkuhn, Arkiv Fysik **23**, 259 (1962).

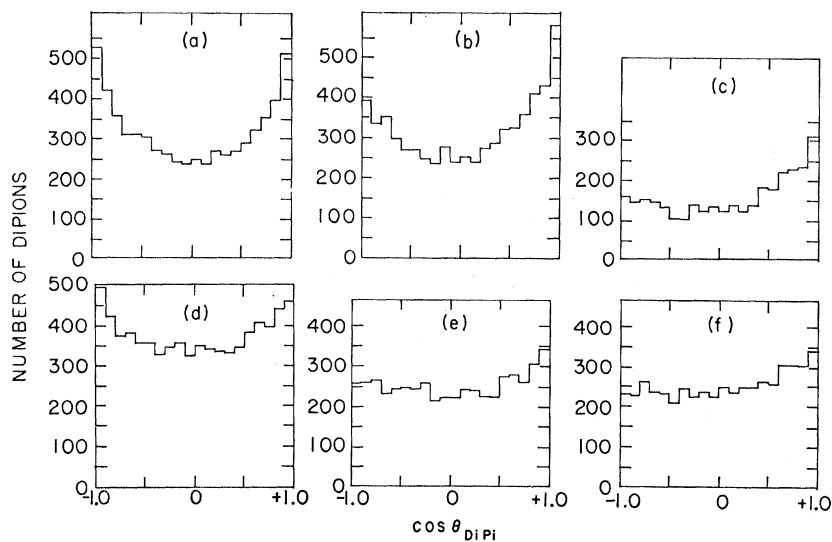


FIG. 4. Production angles of dipions in the center-of-mass system for reactions (5) and (8). The angle for a charged dipion is taken with respect to the similarly charged nucleon. Thus, for dipions of  $T_z=+1$  and  $T_z=+2$  the angle is taken with respect to the proton direction. The angle of the neutral dipion is taken with respect to the antiproton. Dipion distributions shown for reaction (5) are  $T_z=0$  in (a),  $|T_z|=1$  in (b), and  $|T_z|=2$  in (c); and for reaction (8)  $T_z=0$  in (d),  $|T_z|=1$  in (e), and  $|T_z|=2$  in (f).

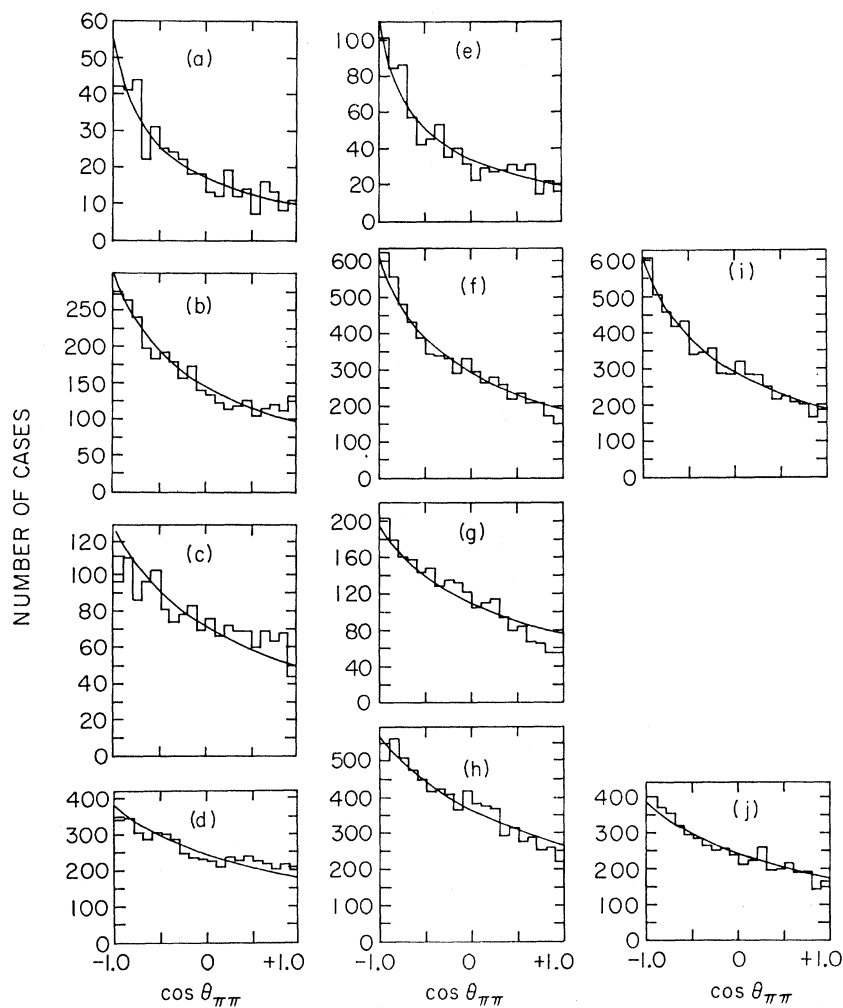


FIG. 5. Distribution of the angle between two pions, the correlation angle  $\theta_{\pi\pi}$ , in the center-of-mass system. Distributions for like-charged pions are shown in (a) for reaction (4), (b) for reaction (5), (c) for reaction (7), and (d) for reaction (8). Distributions for oppositely charged pions are shown in (e) for reaction (4), (f) for reaction (5), (g) for reaction (7), and (h) for reaction (8). Distributions for the neutral-charged pion pairs are shown in (i) for reaction (5) and (j) for reaction (8). The curves shown are the Lorentz-invariant phase-space predictions for the appropriate mixtures of energies and multiplicities.

TABLE IV. Mean values of the angles between pions in the center-of-mass system.

Reaction	Mean value of $\cos\theta_{\pi,\pi}$				
	$\theta_{\pi^{\pm},\pi^{\pm}}$	$\theta_{\pi^+, \pi^-}$	$\theta_{\pi^{\pm}, \pi^0}$	All $\theta_{\pi,\pi}$	Phase space
(4)	$-0.264 \pm 0.028$	$-0.280 \pm 0.020$	...	$-0.275 \pm 0.016$	$-0.267$
(5)	$-0.165 \pm 0.010$	$-0.194 \pm 0.007$	$-0.206 \pm 0.007$	$-0.193 \pm 0.005$	$-0.187^a$
(6)	$-0.127 \pm 0.011$	$-0.125 \pm 0.008$	...	$-0.125 \pm 0.006$	$-0.132^a$
(7)	$-0.100 \pm 0.015$	$-0.198 \pm 0.012$	...	$-0.159 \pm 0.007$	$-0.153$
(8)	$-0.091 \pm 0.008$	$-0.139 \pm 0.007$	$-0.143 \pm 0.008$	$-0.126 \pm 0.004$	$-0.127^a$
(9)	$-0.097 \pm 0.012$	$-0.118 \pm 0.010$	...	$-0.110 \pm 0.005$	$-0.101^a$

<sup>a</sup> Assumes an average multiplicity of 5.2, 6.9, 7.1, and 8.6 pions for reactions (5), (6), (8), and (9), respectively.

$\theta_a$  show the same characteristic anisotropy observed in the case of single pions. Table III summarizes the forward-background and polar-equatorial comparisons for the dipion spectra.<sup>18</sup>

### B. Pion Correlation Angles in the Center-of-Mass System

Figure 5 shows distributions for the angle between two pions in the center-of-mass system (correlation angle  $\theta_{\pi,\pi}$ ). The smooth curves are predictions of Lorentz-invariant phase space. Data from the four-pronged final states are in general agreement with the phase-space curves. However, deviations from phase space occur in the expected regions; that is, for like-charged pions small  $\theta_{\pi,\pi}$  are preferred while for unlike-charged pions large  $\theta_{\pi,\pi}$  are preferred. The differences between like-charged and unlike-charged spectra are more striking in the six-pronged than in the four-pronged events, but they are also significant in the four-prongs. For example, a  $\chi^2$  test of the hypothesis that both of the unlike-charged spectra from reaction (5) came from the same statistical sample gives a 25% confidence level. A similar test for the consistency of  $\theta_{\pi^+, \pi^-}$  with  $\theta_{\pi^{\pm}, \pi^{\pm}}$  indicates that the probability that these two distributions are the same is only about 0.01%. This effect in the pion correlation angles has been interpreted in terms of Bose statistics.<sup>19</sup> Table IV presents the mean values of  $\cos\theta_{\pi,\pi}$  along with the values expected from phase space. The deviations from the values expected according to Lorentz-invariant phase space are smaller at this energy than those observed at lower antiproton momenta.<sup>13,19</sup> This trend is

TABLE V. Decay angular distributions for  $\pi^+\pi^-$  dipions near the  $\rho^0$ -meson mass for reaction (5). Form of distribution  $= 1 - a \cos\theta_{\pi,a} - b \cos^2\theta_{\pi,a}$ .

Mass region (MeV)	$a$	$b$
600-700	$0.10 \pm 0.08$	$0.18 \pm 0.13$
700-800 ( $\rho^0$ )	$0.16 \pm 0.07$	$0.50 \pm 0.10$
800-900	$0.12 \pm 0.09$	$0.01 \pm 0.18$

<sup>18</sup> There does not appear to be any statistically significant correlation between the invariant mass of a dipion or tripion combination and its production angle in the center-of-mass system.

<sup>19</sup> G. Goldhaber, S. Goldhaber, W. Lee, and A. Pais, Phys. Rev. **120**, 300 (1960).

consistent with a model of the type discussed in Ref. 19. An interesting result in regard to the correlation-angle distributions is that the average of  $\cos\theta_{\pi,\pi}$  for all charge combinations in each of the reactions listed in Table IV is in excellent agreement with the phase-space predictions.

### C. Decay Angular Distributions of Dipions

A study of the decay of a dipion in its own rest frame can in principle furnish valuable information regarding the spin of the dipion system. In annihilations there is no clearly preferable choice for the quantization direction; we have used the direction of the line of flight of the dipion in the center-of-mass system. For doubly charged dipions the distributions in  $\theta_{\pi,a}$  must be folded about  $\theta_{\pi,a} = 90^\circ$  because the pions are indistinguishable. For singly charged dipions we have examined the direction of the  $\pi^+$  with respect to the  $(\pi^+, \pi^0)$  dipion line of flight and for the  $\pi^-$  with respect to the  $(\pi^-, \pi^0)$  dipion line of flight. Distributions in  $\theta_{\pi^+, a^+}$  and  $\theta_{\pi^-, a^-}$  were added since they must be the same if  $C$  invariance holds for the annihilation process. A distinction had to be made between neutral  $(\pi^+, \pi^-)$  dipions according to whether they were emitted forward or backward in the center-of-mass system. For  $(\pi^+, \pi^-)$  dipions emitted in the forward direction we examined  $\theta_{\pi^+, a}$  while for the  $(\pi^+, \pi^-)$  dipions emitted in the backward direction we examined  $\theta_{\pi^-, a}$ .<sup>20</sup> The decay distributions for neutral and singly-charged dipions tend to be peaked in the equatorial region ( $\theta_{\pi,a} = 90^\circ$ ) and are more backward than forward. These distributions show rapid fluctuations in the mass region near the  $\rho$  meson when there is a substantial amount of  $\rho$  production. In reaction (5), for example, the  $\rho^0$ -meson production rate is particularly high. Table V gives the form of the distributions needed to describe the decay spectra for  $\pi^+\pi^-$  pairs in reaction (5) when these are studied as a function of the mass of the dipion system. It is clear that a significantly larger  $\cos^2\theta_{\pi,a}$  term is required at the  $\rho^0$  mass (700 to 800 MeV) than in the neighboring regions. The observed asymmetry is similar to the effect noted in off-shell

<sup>20</sup> These steps are necessary for observing forward-backward asymmetries in the decay of neutral dipions in  $\beta$ - $\beta$  annihilations (see Ref. 11). We wish to thank Professor Larry Rosenson for a discussion of this point.

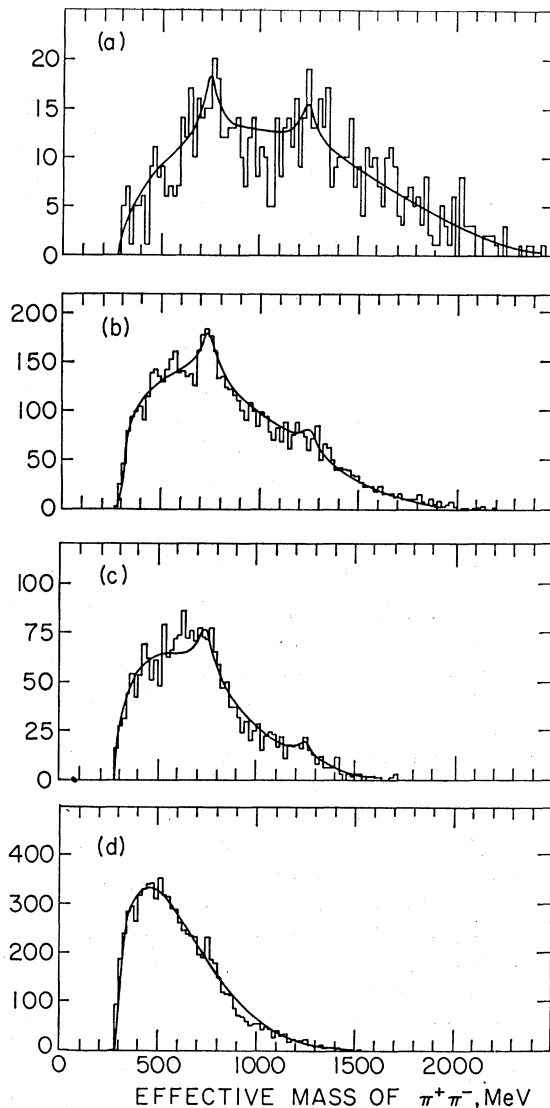


FIG. 6. Effective-mass distributions for  $\pi^+\pi^-$  pair combinations. Shown are (a) 216 events of reaction (4), (b) 1596 events of reaction (5), (c) 255 events of reaction (7), and (d) 904 events of reaction (8). The comparison curves shown in (a), (b), and (c) are phase space to which Breit-Wigner shaped resonances representing the  $\rho^0$  and  $f^0$  mesons have been added incoherently. Only phase space appears in (d). Contamination has been treated by the inclusion of phase space for three pions from the reaction having an extra  $\pi^0$ ; however, the effect of the fitting procedure has not been taken into account.

$\pi^+\pi^-$  scattering.<sup>21</sup> The charged- $\rho$  mass region also shows an asymmetry in  $\theta_{\pi,d}$ . It is not clear whether this asymmetry in  $\rho^0$  or in  $\rho^\pm$  decay is a property of the background alone or if it is associated as well with the  $\rho$  meson. The decay of doubly charged dipions is consistent with isotropy.

<sup>21</sup> See, for example, V. Hagopian, W. Selove, J. Alitti, J. P. Baton, and M. Neveu-Rene, *Phys. Rev. Letters* **14**, 1077 (1965). We wish to point out that the interpretation of  $\theta_{\pi,d}$  is further complicated by the large combinatorial background in the  $p$ - $p$  annihilations.

## IV. INVARIANT-MASS DISTRIBUTIONS

### A. Resonance Production

We have examined all invariant-mass combinations for the reactions listed in Table I. Only the  $\rho$  and  $\omega^0$  mesons were observed in significant amounts. There was some evidence for  $f^0$  production. A search for new resonances<sup>22</sup> as well as for the  $A_1$ ,  $A_2$ , and  $B$  resonances<sup>23</sup> proved unsuccessful.

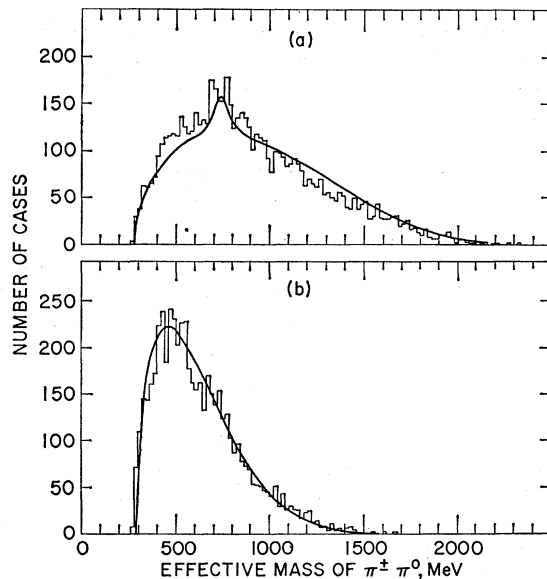


FIG. 7. Distributions of the effective mass of  $\pi^+\pi^0$  pair combinations for (a) reaction (5) and (b) reaction (8). The smooth curve in (a) is an incoherent addition of Lorentz-invariant phase space and a Breit-Wigner shape for the  $\rho^\pm$  meson, while that shown in (b) is phase space alone. The fit to the background is not good because we have not considered the effect of the kinematic fitting process on events which have in fact more than one missing  $\pi^0$ . Some multineutral events give acceptable fits to reaction (5) because of the large measuring errors. These false events can have characteristics which are different from those of the true events in the sample. Hence when distributions involving the  $\pi^0$  are studied particularly severe distortions of the spectra can be expected.

<sup>22</sup> T. Ferbel, J. Sandweiss, H. D. Taft, M. Gailloud, T. W. Morris, W. J. Willis, A. H. Bachman, R. M. Lea, and P. Baumel, (unpublished). This report presents results of a control experiment which was performed in order to determine the statistical significance of an enhancement observed in the  $\pi^+\pi^-$  system at a mass of  $\sim 560$  MeV. The initial effect (approximately four standard deviations enhancement above phase space) was observed in the  $\pi^+\pi^-$  mass spectrum of reaction (5). This enhancement was associated primarily with those events which contained a charged pion emitted in the forward direction in the center-of-mass system ( $\cos\theta_\pi > 0.9$ ). In the control experiment no enhancement was observed at 560 MeV; on the basis of the number of events observed at 560 MeV we concluded that the effect in the main sample of data was a statistical fluctuation. We wish to thank Professor Arthur H. Rosenfeld for his criticism and many interesting discussions concerning these data.

<sup>23</sup> A. H. Rosenfeld, A. Barbaro-Galtieri, W. H. Barkas, P. L. Bastien, J. Kirz, and M. Roos, *Rev. Mod. Phys.* **36**, 977 (1964). This paper gives an exhaustive list of references for the production and characteristics of newly discovered resonances.

TABLE VI. Cross sections for resonance production (mb).

Reaction	$\rho^0$	$\rho^\pm$	$f^0$	$\omega^0 \rightarrow \pi^+\pi^-\pi^0$	$\eta^0 \rightarrow \pi^+\pi^-\pi^0$
(2)	<0.05	<0.05	...	...	...
(4)	$0.2 \pm 0.1$	...	$0.1 \pm 0.1$	...	...
(5)	$1.3 \pm 0.3$	$1.0 \pm 0.3$	$0.6 \pm 0.3$	$0.4 \pm 0.1$	<0.03
(7)	$0.9 \pm 0.3$	...	$0.2 \pm 0.1$	...	...
(8)	$0.5 \pm 0.2$	$0.2 \pm 0.2$	...	$0.8 \pm 0.2$	<0.2

As at lower energies<sup>24</sup> reactions (4), (5), (7), and (8) proceed a major portion of the time through *single* resonance production. That is, although resonances are produced profusely there is no evidence for double resonance production in antiproton-proton annihilations.<sup>3</sup>

Several mass spectra are presented in Figs. 6 through 9. The comparison curves are incoherent admixtures of Lorentz-invariant phase-space predictions with *s*-wave Breit-Wigner functions for wide resonances, and Gaussians for resonances whose widths are narrower than the experimental resolutions. We have assumed throughout that the effect of resonance production on

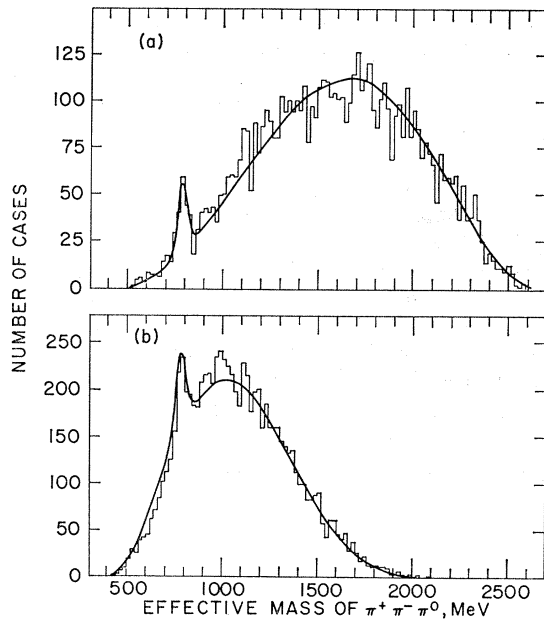


FIG. 8. Effective-mass distributions for the  $\pi^+\pi^-\pi^0$  combinations for (a) reaction (5) and (b) reaction (8). The  $\omega^0$  meson has a width less than our resolution and is therefore represented by a Gaussian whose standard deviation is our estimated resolution [35 MeV in (a) and 30 MeV in (b)]. The background is represented by an incoherent mixture of phase space for the given reaction and the phase space for the contamination from the appropriate  $2\pi^0$  final state. The effect of kinematic fitting or the presence of other resonances is not taken into account.

<sup>24</sup> M. Cresti, A. Grigoletto, S. Limentani, A. Loria, L. Peruzzo, R. Santangelo, G. B. Chadwick, W. T. Davies, M. Derrick, C. J. B. Hawkins, P. M. D. Gray, J. H. Mulvey, P. B. Jones, D. Radojicic, and C. A. Wilkinson, in *Proceedings of the Sienna International Conference on Elementary Particles*, edited by G. Bernadini and G. P. Puppi (Società Italiana di Fisica, Bologna, 1963), Vol. I, p. 263. Also see Ref. 13.

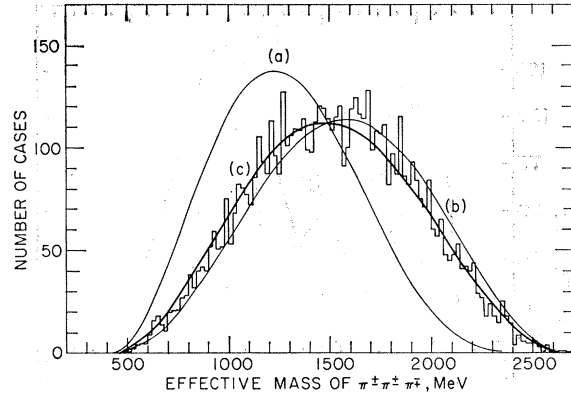


FIG. 9. Distribution of effective mass for the  $\pi^+\pi^+\pi^-\pi^0$  combination from reaction (5). It illustrates the addition of a fraction of six-pion phase space to account for contamination. Curves shown are (a) three pions out of six, (b) three pions out of five, and (c) the combination of 20% of (a) and 80% of (b).

the nonresonant spectra for any given reaction can be neglected. We have, in other words, ignored all reflections of resonances—production as well as decay. Because of the large combinatorial background in these final states, this is not a serious deletion. In general, the nonresonant mass combinations follow phase space remarkably well.<sup>25</sup> The strongest deviations from phase space are found for reaction (7). The  $T_z = \pm 2$  dipion mass spectrum tends to be shifted to lower masses while the  $T_z = 0$  dipion spectrum appears to be shifted to higher masses. Identical effects in this final state have been observed at both lower<sup>13,24</sup> and at higher<sup>14</sup> energies. This shift may be related to the correlation angle observations discussed in the previous section.<sup>26</sup>

Cross sections for the production of resonances in the annihilation data at 3.28 BeV/*c* antiproton momentum are given in Table VI. The combinatorial background in reactions (10), (11), and (12) is too large to make a meaningful measurement of production rates for the resonances given in Table VI.

## B. Missing-Mass Spectra and Multiplicities

Figure 10 shows histograms for the missing mass reactions (6) and (9). We have attempted to determine the average pion multiplicity of the multineutral events by taking varying fractions of phase-space curves for two, three, four, and five missing neutral pions and visually

<sup>25</sup> We have compared our mass-distribution, transverse-momentum, and total-momentum data with the Lorentz-invariant phase space. We have also computed some of the spectra, using a Monte Carlo program, according to the Fermi phase space and found that both theories give adequate fits to the shapes of the distributions. See in this respect R. K. Adair, *Rev. Mod. Phys.* **37**, 473 (1965).

<sup>26</sup> This shift in the  $T_z = \pm 2$  mass spectrum toward smaller masses can be understood on the basis of Bose statistics (see Ref. 19). The fact that similar shifts occur in the eight-pronged data when all the particles in a given mass grouping (two, three, or four) have the same charge makes the Bose statistics explanation appealing.



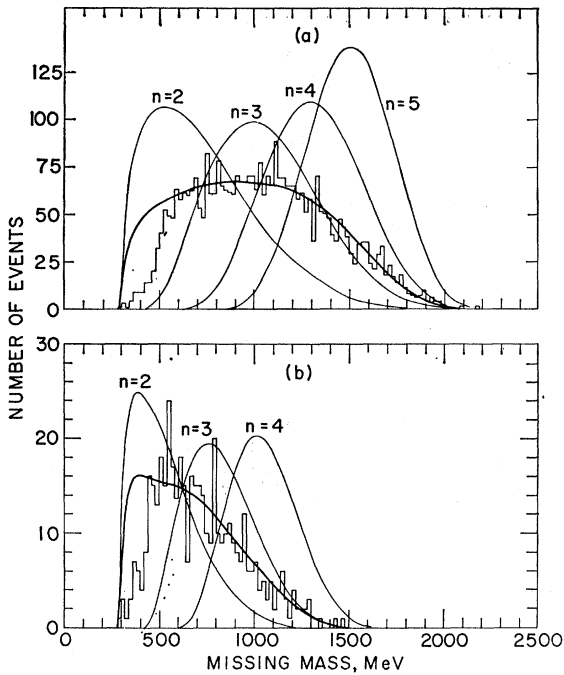


FIG. 10. Distribution of missing masses for reactions (6) and (9). In (a) we show 3556 events of reaction (6). The curves are phase-space spectra for 2, 3, 4, and 5 missing  $\pi^0$  mesons; each curve is normalized to the total number of events. Also shown is a composite curve with weights of 0.50, 0.30, 0.20, and 0.08 for 2, 3, 4, and 5  $\pi^0$  mesons, respectively, normalized to the region above 600 MeV. In (b) we show the missing-mass distribution for 468 events of reaction (9). The curves in (b) represent phase space for 2, 3, and 4 missing  $\pi^0$  mesons, normalized to the total number of events. Also shown is a composite curve with weights of 0.65, 0.35, and 0.10, for 2, 3, and 4  $\pi^0$  mesons, respectively, normalized to the region above 600 MeV.

fitting the resultant composite curve to the regions above 600 MeV. The number of two- $\pi^0$  events which have an invariant mass of 600 MeV or more and which have been incorrectly classified as reactions (5) or (8) is negligible. Hence, if phase space is a good enough approximation, the best combination curve should yield a

TABLE VII. Composition of multineutral events (percent of reaction).<sup>a</sup>

Number of $\pi^0$	Reaction (6)	Reaction (9)
2	46 $\pm$ 5 <sup>b</sup>	59 $\pm$ 5 <sup>b</sup>
3	28 $\pm$ 5	32 $\pm$ 5
4	19 $\pm$ 5	9 $\pm$ 5
5	7 $\pm$ 3	...
Average number	2.9 $\pm$ 0.3 <sup>c</sup>	2.5 $\pm$ 0.3 <sup>c</sup>

<sup>a</sup> Errors indicated in the table are estimates only.

<sup>b</sup> This entry includes the events which could not be resolved from reactions (5) and (8).

<sup>c</sup> Does not contain error due to the uncertainty in the measured cross sections for multineutral channels given in Table I.

reasonable estimate of the multineutral spectrum. Table VII gives the results of the analysis of the multineutral events. This determination is consistent with the multiplicity obtained from similar fits to other effective-mass distributions for the multineutral events. It is also consistent with the previously estimated loss of two- $\pi^0$  events from reactions (6) and (9) because of successful fits to reactions (5) and (8).

From the data in Table I we obtain a charged-pion multiplicity of  $4.0 \pm 0.3$ . Using the average neutral multiplicities given in Table VII and assuming a neutral-pion multiplicity for reaction (3) of 3.5 we have calculated the over-all pion multiplicity in these data; this is  $6.5 \pm 0.5$ . These values are consistent with the trend of the data observed at lower energies.<sup>27</sup>

#### ACKNOWLEDGMENTS

We wish to thank Dr. R. P. Shutt and the many individuals of the BNL Bubble Chamber Group whose efforts have made this experiment possible. We also wish to thank Professor Ted Kalogeropoulos for his contributions in the early stages of this experiment. Finally we acknowledge the many enjoyable and fruitful conversations we have had with Professor Joseph Shpiz.

<sup>27</sup> G. R. Lynch, Rev. Mod. Phys. 33, 395 (1961).